

A New Method for Chill and Shrinkage Control in Ladle Treated Ductile Iron

T.Skaland

Elkem Foundry Products, Kristiansand, Norway

ABSTRACT

The present paper is undertaken with the objective of describing a new method for treating ductile cast iron in a ladle process, where the main objective is to minimize formation of eutectic carbides and shrinkage porosity during solidification.

The suppression of carbide formation is associated with the nucleating properties of the nodularizer and inoculant alloys. By nucleating properties it is understood the number and potency of nuclei formed by an alloy addition. The nodularizer and inoculant additions also influence ductile iron solidification shrinkage. Some alloys may give good protection against shrinkage while others tend to promote more shrinkage. The use of various rare earth elements is found to have a pronounced impact on these conditions.

It has been discovered that the use of pure lanthanum as the primary rare earth source in the magnesium ferrosilicon nodularizer surprisingly further improves the performance of the ductile iron ladle treatment method compared to similar methods using cerium or misch metal bearing nodularizers. The nucleating properties are substantially improved and the risk for chill and shrinkage formation in the sandwich or tundish ladle treated ductile iron is then minimized.

The paper describes this new ladle treatment concept in detail, and gives examples from successful testing of the new nodularizing technology and how it simultaneously affects and minimizes critical ductile iron chill and shrinkage tendencies.

INTRODUCTION

The scope of the present work is to study the effects of lanthanum and cerium bearing MgFeSi alloys used in ladle treatment of ductile iron on the microstructure evolution, graphite morphology and solidification shrinkage in ductile irons produced under controlled laboratory conditions.

BACKGROUND

Previous investigations have shown that rare earth metals (REM) such as cerium, lanthanum, praseodymium and neodymium can either have a beneficial or a detrimental effect on the microstructure and properties of ductile iron, depending on the casting conditions. For example, small additions of REM are frequently used to restore the graphite nodule count and nodularity in ductile irons containing subversive elements such as Sb, Pb, Ti etc.¹⁻³ On the other hand, rare earths in excessive concentrations may lead to problems with chill formation in thin cast sections and chunky graphite in heavier sections, with subsequent degradation in the mechanical properties.⁴⁻⁶

Several investigators have reported an optimum level of REM with respect to a high nodule count and reduced carbide formation. However, the optimum rare earth content varies significantly according to different investigators. For example, Lalich⁷ concluded that the optimum cerium level is about 0.006 to 0.010 wt% for low cerium rare earth's, and about 0.015 to 0.020 wt% for high cerium rare earth's, while Kanetkar et al⁸ found a maximum nodule count at a cerium concentration of 0.032 wt%. The lowest values as reported by Lalich⁷ are close to the residual level of cerium in commercial irons, and seem therefore difficult to control in practice. Kanetkar et al⁸ also reported that separate additions of lanthanum, praseodymium and neodymium produce an optimum nodule count at a certain concentration level of each element. The residual contents required for an optimum nodule count were as follows: 0.018% for lanthanum, 0.007-0.010% for praseodymium, and 0.017% for neodymium. Similar values for cerium and lanthanum were also reported by Onsøien et al⁹, i.e. 0.035% cerium and 0.017% lanthanum.

Graphite type, size and shape formed during ductile iron solidification, as well as the amount of graphite versus iron carbide, can be controlled with certain additives that promote the formation of graphite during solidification of cast iron. These additives are referred to as nodularizers and inoculants and their addition to the cast iron as nodularizing and inoculation. In casting iron products from liquid iron, there will always be a risk for the formation of iron carbides in thin sections of castings.

The formation of iron carbide is brought about by the rapid cooling of the thin sections as compared to the slower cooling of the thicker sections of the casting. The formation of iron carbide in a cast iron is referred to as "chill" and is quantified by measuring "chill depth". The power of a nodularizer or inoculant to prevent chill and reduce chill depth is a convenient way to measure and compare the individual power of different nodularizers and inoculants.

Since the exact chemistry and mechanism of nucleation and why nodularizers and inoculants function as they do is not completely understood, a great deal of research goes into providing the industry with new and improved alloys. The suppression of carbide formation is associated with the nucleating properties of the nodularizer and inoculant. By nucleating properties it is understood the number of nuclei formed by an alloy addition. A high number of nuclei improves the effectiveness of the carbide suppression. Further a high nucleation rate may also give better resistance to fading effects during prolonged holding time of the molten iron after nodularizing and inoculation.

The nodularizer and inoculant alloys also affect ductile iron solidification shrinkage. Some alloys may give good protection against shrinkage while others tend to promote more shrinkage. The use of various rare earth elements may have a pronounced impact on this condition. For nodularizer alloys it is also important that composition of the alloy is such that a minimum of shrinkage occurs during solidification of the iron.

The nodularizing process is carried out in two basically different ways. In the so-called "ladle treatment method", the nodularizer alloy is placed in the bottom of the ladle whereafter liquid cast iron is poured into the ladle on the top of the nodularizer alloy. Depending on how the nodularizer alloy is placed in the ladle, the ladle treatment method is known as overpour, sandwich, or tundish cover treatment methods. Inoculation is normally carried out after the nodularizing process is done, by adding inoculant to the metal stream during transfer of the cast iron to a pouring vessel or to a mould.

In the so-called "in-the-mould" method, the nodularizing treatment is taking place inside the mould cavity itself. The in-the-mould nodularizing method is thus significantly different from the ladle treatment nodularizing method.

According to Dunks¹⁰, the addition of pure lanthanum with magnesium ferrosilicon alloy has proven successful for the purpose of minimizing chill and shrinkage in ductile iron when using the in-the-mould nodularizing method. In the in-the-mould treatment method, the

magnesium ferrosilicon alloy acts both as a nodularizer and inoculant simultaneously integrated into the gating system of the mould. For magnesium treatment of cast iron in the ladle treatment nodularizing method, such integrated or combined nodularizing and inoculation is not yet known.

MATERIALS AND EXPERIMENTAL WORK

Ductile iron heats were produced in an induction furnace from a charge based on 50 wt% steel, 20 wt% iron returns and 30 wt% pig iron. Carbon and silicon were adjusted using graphite recarburizer and ferrosilicon. Prior to tapping into the treatment ladle, 1.5 wt% magnesium ferrosilicon alloy was placed into the ladle and covered by 0.5 kg steel punchings, i.e. nodularizing according to the sandwich treatment method. **Figure 1** shows a schematic representation of the type of tundish/sandwich treatment ladles used. Two minutes after treatment the iron was transferred into the pouring ladle. No post-inoculant has been added after the nodularizing treatment, thus the experimental irons are cast into the sand moulds in un-inoculated condition. This is done to only reveal the characteristic effects of the individual nodularizing alloys. Coin shaped samples for chemical analysis were extracted from the melt, and the ductile iron was then cast into sand moulds to produce a 20 mm thick plate, a 5 mm thin plate, a chill wedge sample and a cross bar sample for shrinkage evaluation. The target final composition was 3.7%C, 2.4%Si, 0.4%Mn, 0.010%S and 0.040%Mg.

Table 1 shows the chemical composition of the different magnesium ferrosilicon alloys used in this experimental work. The alloys are based on 45% FeSi with about 6%Mg, 1%Ca, and 0.9%Al. The rare earth content is varied according to **Table 1**. Pure lanthanum at 0.5% and 1.0% as well as pure cerium at 0.5% and 1.0% are compared to a RE-free reference alloy and a conventional 1.0%RE bearing alloy where the rare earth is present as 50% cerium bearing Misch metal.

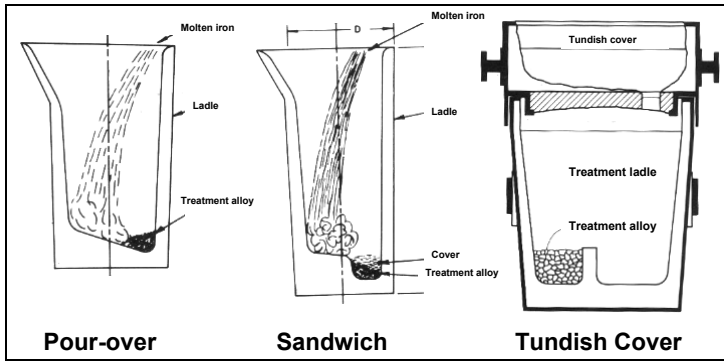


Figure 1: Examples of overpour, sandwich and tundish cover ladles.

Table 1: Chemical composition of magnesium ferrosilicon nodularizer alloys.

Nodularizer	%Si	%Mg	%Ca	%Al	%RE	%Ce	%La
RE-free	45.8	6.1	1.0	0.9	0.0	0.0	0.0
0.5% La	45.0	5.8	1.0	0.9	0.5	0.0	0.5
1.0% La	45.5	6.0	1.0	0.9	1.0	0.0	1.0
0.5% Ce	45.6	6.1	1.0	0.9	0.5	0.5	0.0
1.0% Ce	45.4	6.1	0.9	0.9	1.0	1.0	0.0
1.0% MM	45.0	5.9	1.1	0.8	1.0	0.5	0.25

%RE is the total rare earth content (sum of Ce, La, Pr, and Nd). Balance iron.

Thermal analyses were performed for each heat using samples extracted from the melt in the pouring ladle. Liquid metal was poured into a standard Quick-cup and the cooling curve recorded using the Novacast ATAS® Verifier 4.0 software for analysing characteristic temperature data. The following parameters were extracted from ATAS for comparison: low eutectic temperature (TE_{low}), high eutectic temperature (TE_{high}), final solidification temperature (TS), recalescence (R), graphite factor 1 (GRF1), and graphite factor 2 (GRF2).

Chemical analysis of chilled coin shaped specimen was performed using XRF. The coin samples were also used for determination of carbon and sulphur contents by Leco, and magnesium concentration by AAS. Samples were taken from all treated pouring ladles.

Samples for metallographic examination were extracted from a cross section cut through the centre of the 5 mm and 20 mm plates. The metallographic samples were prepared according to standard metallographic techniques, i.e. polished to a 1 μ m diamond spray finish for characterisation of the graphite. The graphite phase was characterized using an image analysis system (ImagePro Plus). For analysis of graphite particle parameters, only the graphite nodules larger than 5 μ m

were measured. The following data was recorded: nodule count, area fraction of graphite, nodule diameter, nodule shape factor, and nodularity, where nodularity is the percent of graphite nodules with a shape factor better than 0.65. The polished samples were then etched in 2% Nital for automatic image analysis quantification of the microstructure constituents i.e. ferrite, pearlite and carbides.

Chill was evaluated by means of a standard chill wedge sample. Two features were measured, L1 which is the maximum distance, in mm, at which chill is formed in the whole cross section of the chill wedge sample (clear chill), and L2 which is the maximum distance at which carbides are found (total chill).

The crossbar specimens were cut horizontally in a section through the center of the cross to evaluate shrinkage porosity. The specimens were ground and polished to a 1 μ m diamond spray finish, and porosity measured in a reference area of 12 by 12 mm manually positioned at the center of the cross. An image analysis system (ImagePro Plus) was used to quantify the area fraction of porosity in the section relative to the reference area.

RESULTS AND DISCUSSION

Chemical Analysis

Results from chemical analyses of the different heats are summarized in **Table 2**. It is clear that the targeted final composition of 3.7%C, 2.4%Si, 0.4%Mn, 0.010%S and 0.040%Mg is quite well obtained for all experimental heats.

Variations in cerium and lanthanum analyses are projecting the different input of these two elements from the individual MgFeSi alloys applied. Cerium ranges from residual level up to 0.016%, while lanthanum ranges from residual up to 0.015% in the experimental series.

Microstructure

Results from metallographic evaluation of graphite structures are shown in **Table 3**. Microstructures of the test castings are shown in **Figures 2** and **3**, for the 5 and 20 mm plate sections, respectively. **Figure 4** shows histograms for nodule count, nodularity, average nodule diameter, as well as pearlite content for the 20 mm section plate samples.

Table 2: Chemical composition of the produced experimental ductile iron castings.

Nodularizer	%C	%Si	%Mn	%P	%S	%Mg	%Ce	%La
RE-free	3.73	2.51	0.46	0.027	0.009	0.046	<0.004	<0.004
0.5% La	3.75	2.28	0.43	0.020	0.008	0.043	<0.004	0.008
1.0 % La	3.73	2.25	0.42	0.024	0.010	0.040	<0.004	0.015
0.5% Ce	3.70	2.38	0.45	0.020	0.007	0.041	0.010	0.005
1.0 % Ce	3.71	2.35	0.45	0.021	0.008	0.045	0.016	0.007
1.0% Misch	3.74	2.37	0.45	0.021	0.008	0.047	0.010	0.005

Table 3: Characteristic graphite data for cast 5 and 20 mm plate sample sections.

Nodularizer alloy	5 mm plates				20 mm plates			
	Nodule count (N/mm ²)	Nodularity (%)	Average diameter (μm)	Average Shape Factor	Nodule count (N/mm ²)	Nodularity (%)	Average diameter (μm)	Average Shape factor
RE-free	110	81	9.3	0.75	112	42	20.2	0.50
0.5%La	595	93	13.4	0.88	224	78	17.5	0.74
1.0%La	488	93	13.2	0.88	188	69	19.1	0.67
0.5%Ce	164	73	13.1	0.70	148	55	24.3	0.59
1.0%Ce	177	75	15.4	0.72	149	60	23.1	0.64
1.0%MM	418	93	14.8	0.86	178	69	20.8	0.67

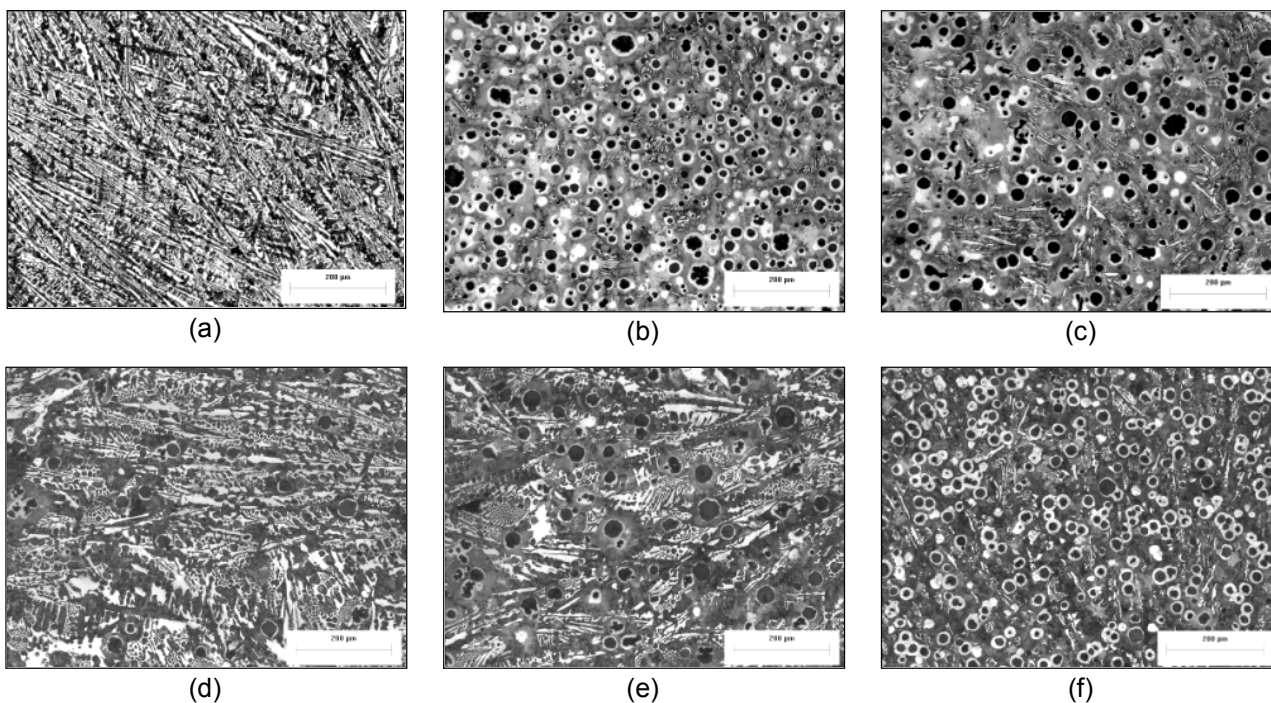


Figure 2: Microstructure in 5 mm plate castings for the different nodularizer alloys. (a) RE-free, (b) 0.5%La, (c) 1.0%La, (d) 0.5%Ce, (e) 1.0%Ce, (f) 1.0%MM.

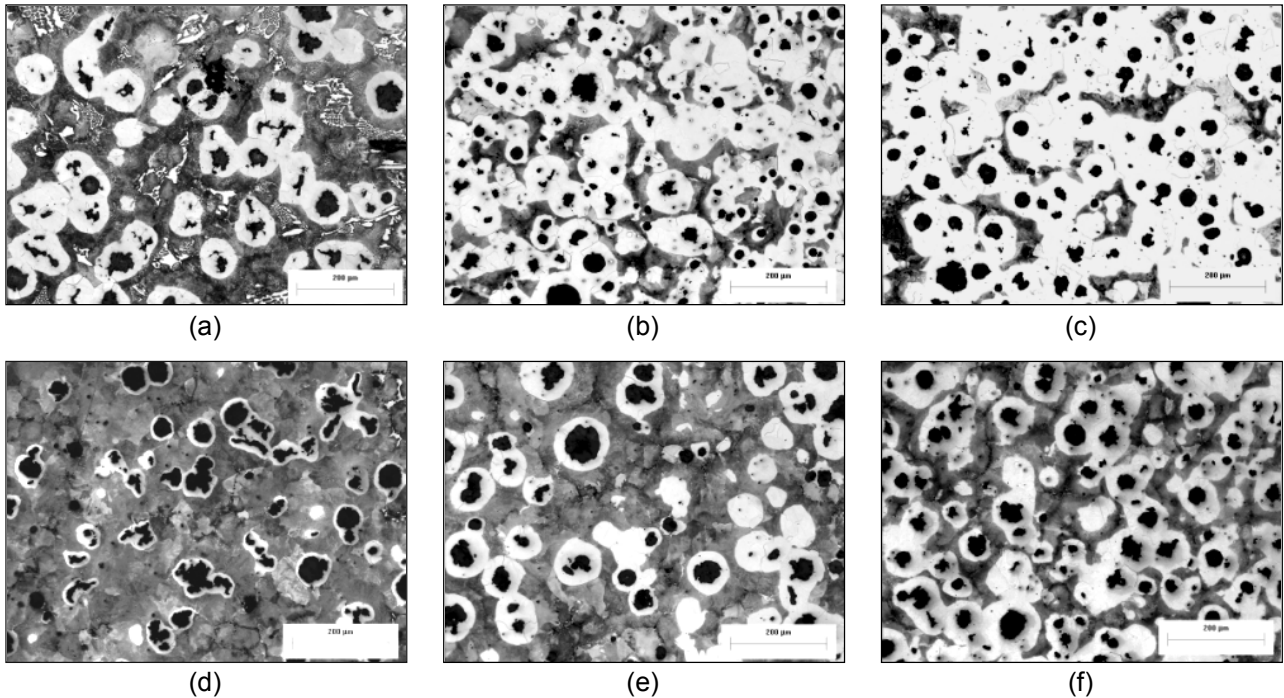


Figure 3: Microstructure in 20 mm plate castings for the different nodularizer alloys. (a) RE-free, (b) 0.5%La, (c) 1.0%La, (d) 0.5%Ce, (e) 1.0%Ce, (f) 1.0%MM.

Nodule count

From **Table 3** and **Figure 4** it is seen that a substantial increase in the number of nodules occurred in the two test heats using pure lanthanum compared to those using rare earth free, cerium and misch metal containing MgFeSi alloys, respectively. This is observed in the 20 mm plates and, especially, in the 5 mm plates.

Nodularity

Nodularity is also found to be higher for the lanthanum treated irons. In the 5 mm plate, 93% nodularity is obtained for lanthanum and mischmetal based MgFeSi alloys, while the cerium based alloys only gave about 75% nodularity. In the 20 mm plates, the 0.5% lanthanum alloy gave the highest nodularity (78%), while the equivalent 0.5% cerium based alloy gave only 55% nodularity.

Pearlite content

The pearlite content in the 20 mm plates varies substantially between the different heats. The lowest pearlite content is found for the 1% lanthanum alloy at only about 25% pearlite. The highest pearlite content is found for the 0.5% cerium alloy at about 75% pearlite. **Figure 4(d)** shows pearlite content for all 20 mm test plates.

Nodule size distribution

Figure 5 shows the nodule size distribution histograms for the 20 mm plates for all heats. It is evident that there are significant differences in nodule size distribution between the lanthanum and cerium bearing nodularizers. The two lanthanum bearing cases in **Figures 5(b)** and **(c)** shows a more skewed nodule distribution to smaller sizes than the cerium bearing cases in **Figures 5(d)** and **(e)** where the size distribution is much flatter.

Figure 5(f) shows that the 1% mischmetal bearing nodularizer also gives a somewhat skewed nodule size distribution, but not as skewed as the pure lanthanum bearing alloys. The RE-free nodularizer in **Figure 5(a)** shows a flat nodule size distribution more comparable to the pure cerium cases.

The nodule size distribution affects shrinkage tendency, since it reflects graphite formation and expansion throughout the entire solidification sequence. Small nodules and skewed distributions suggest late graphite formation and thus good protection against micro-porosity at the very end of solidification. Larger nodules and a flat distribution suggest more early graphite expansion and less effect at the end, resulting in an elevated risk for micro-porosity.

Chilling tendency

From **Figures 2(b)** and **(c)** it is seen that the lanthanum containing magnesium ferrosilicon alloys strongly reduces and nearly eliminates chill carbides in the 5 mm plates, and that no chill can be found in the 20 mm plates as shown in **Figures 3(b)** and **(c)**.

The pure cerium bearing alloys, **Figures 2(d)** and **(e)**, resulted in substantial chilling in the 5 mm plate, while the 1% mischmetal containing alloy, **Figure 2(f)**, only gave moderate carbide formation in this plate section. The RE-free nodularizer, **n Figure 2(a)**, resulted in a fully white 5 mm casting section and a mixed carbide-graphite structure in the 20 mm plate section shown in **Figure 3(a)**.

Results from measurements of clear chill width in the cast wedge samples are reported in **Figure 7(b)**. This histogram shows that the RE-free nodularizer and the two pure cerium bearing nodularizers gave fully white wedge samples all the way to the top of the wedge (50 mm). The lanthanum bearing nodularizers gave the

smallest chill at only about 11 to 12 mm, while the mischmetal bearing alloy resulted in about 14 mm chill in the wedge.

Shrinkage porosity

Table 4 and **Figures 6(b)** and **(c)** show that shrinkage porosity is totally eliminated when using the pure lanthanum bearing MgFeSi alloys. Both pure cerium bearing alloys in, **Figures 6(d)** and **(e)**, show indications of scattered micro-porosity in the structure with about 2% pore volume measured in both cases.

The 1% mischmetal containing alloy in **Figure 6(f)** shows a large shrinkage cavity, resulting from primary shrinkage effects during solidification.

Figure 6(a) shows substantial scattered micro-porosity found in the RE-free nodularizer sample. **Figure 7(d)** shows a histogram representing relative shrinkage volumes for all samples tested.

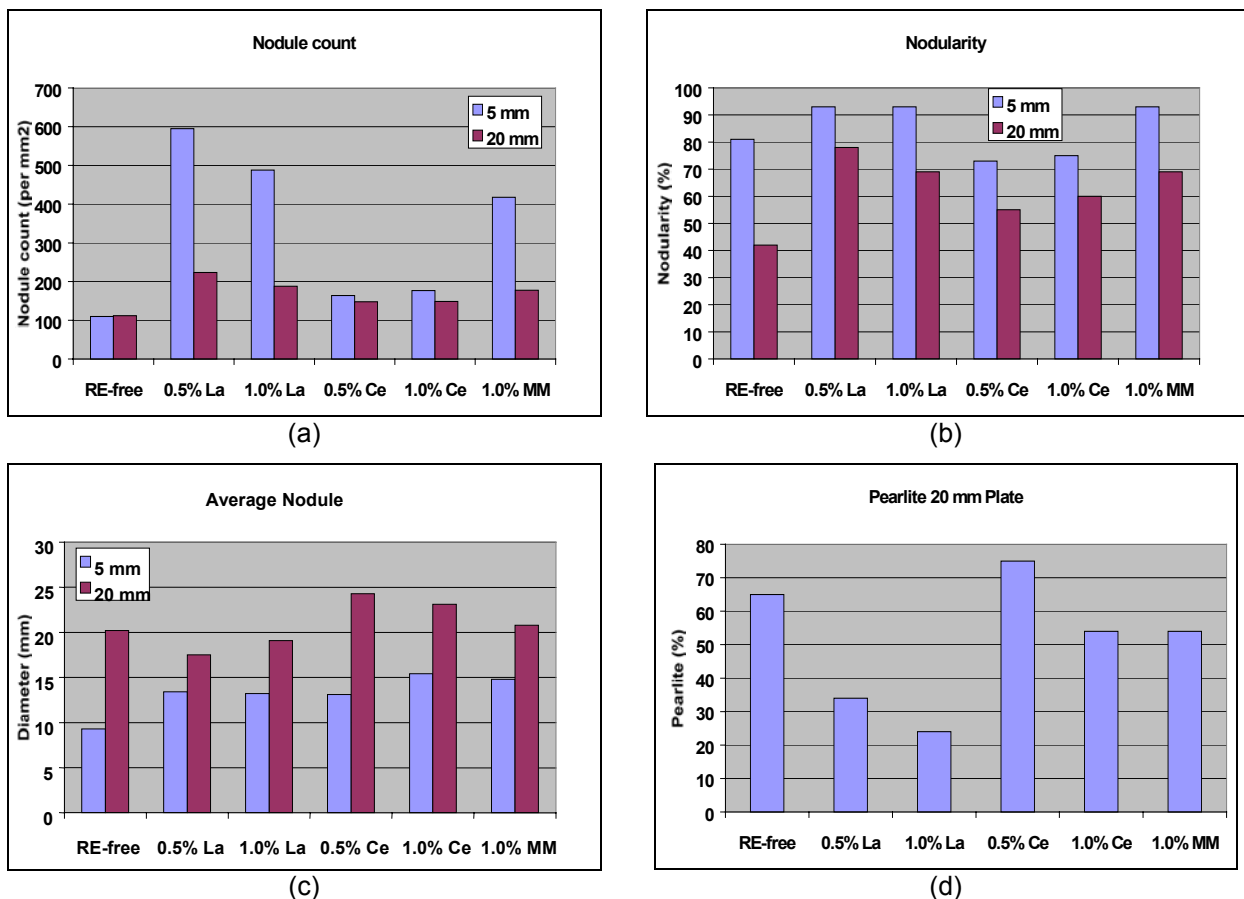


Figure 4: Microstructure parameters as a function of nodularizer alloy for the 5 and 20 mm plates. (a) nodule count, (b) nodularity, (c) average nodule diameter, (e) pearlite content (20 mm plate only).

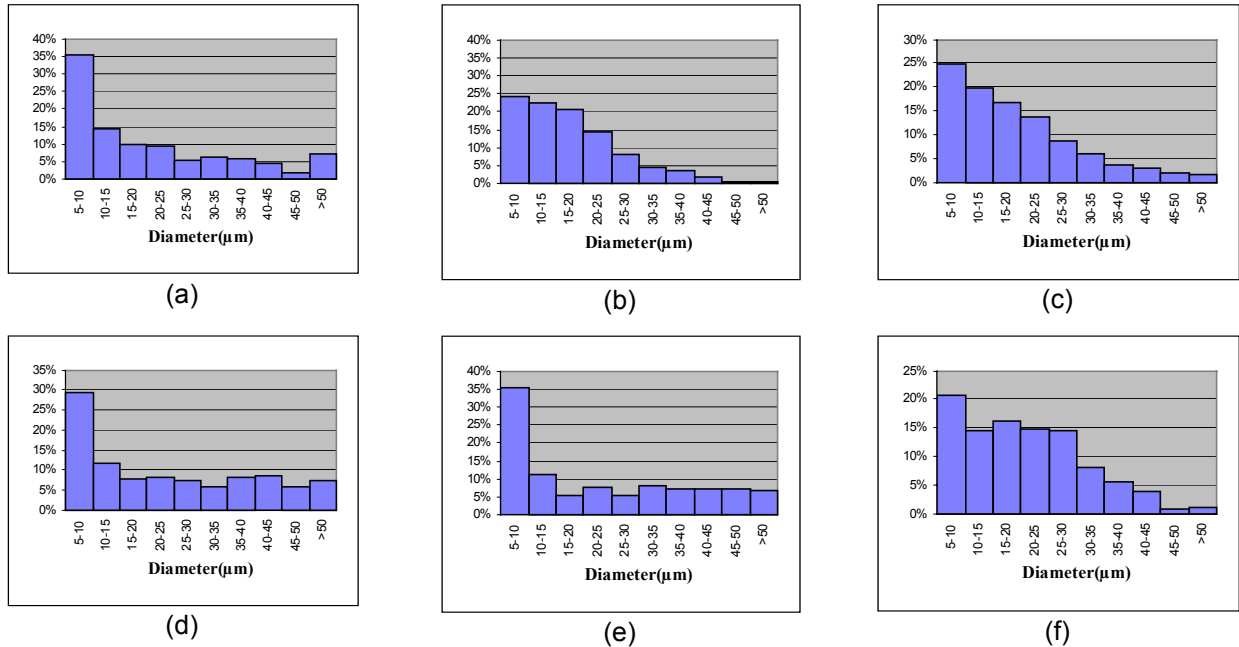


Figure 5: Nodule size distribution for the different nodularizer alloys. (a) RE-free, (b) 0.5%La, (c) 1.0%La, (d) 0.5%Ce, (e) 1.0%Ce, (f) 1.0%MM.

Table 4: Relative shrinkage porosity area in crossbar castings.

Nodularizer	Area % pores
RE-free	8.3
0.5% La	0.0
1.0% La	0.0
0.5% Ce	2.3
1.0% Ce	2.0
1.0% Misch	38.2

Because of the low chill and shrinkage formation tendencies, especially for the 0.5% lanthanum containing magnesium ferrosilicon alloy, the need for a subsequent addition of post inoculant material is minimized or may even be eliminated. Thus, the lanthanum-bearing MgFeSi alloy ladle treatment process represents a unique new nodularizing method that will be cost effective also in the sense that a minimum requirement for inoculation performance is needed.

Thermal analysis data

Thermal analysis performed on each heat using the ATAS® Verifier 4.0 software shows some important differences between the cooling curves of the individual nodularizers tested.

Figure 7(a) shows the characteristic temperatures from ATAS; T_{low}, T_{high}, and T_S, representing low

eutectic, high eutectic, and end of solidification temperatures, respectively.

It is seen from **Figure 7(a)** that the highest temperatures are recorded for the 0.5% lanthanum bearing alloy, suggesting the highest resistance towards chill and shrinkage formation. The lowest TS temperatures are recorded for the cerium bearing alloys as well as the RE-free alloy. Low TS is an indication of high microshrinkage formation tendency. These observations from thermal analysis temperature measurements correspond well with the actual measurements of chill and shrinkage in the present casting samples, see **Figures 7(b)** and **(d)**.

Figure 7(c) shows a histogram for the characteristic graphite factors 1 and 2 (GRF1 and GRF2) from the ATAS thermal analysis. These factors give important information about shrinkage tendency. A large GRF1 and a small GRF2 are desired for minimum shrinkage formation tendency. It is found that the two pure lanthanum-bearing alloys give the highest GRF1 values at about 95 to 100, and the lowest GRF2 values at about 30-35. The inverse situation is found for the pure cerium bearing alloys.

These observations from the graphite factor measurements correspond well with the actual measurements of shrinkage in the present casting samples, see **Figure 7(d)**.

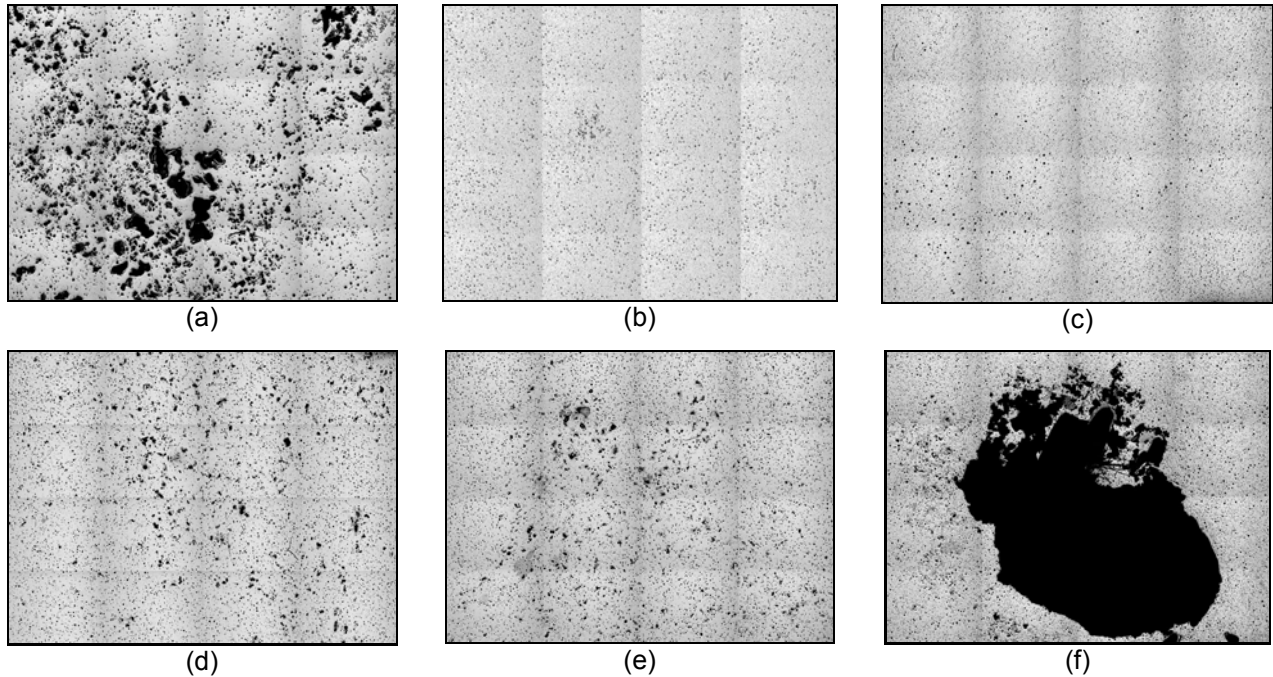


Figure 6: Shrinkage porosity in section cut through the crossbar casting for different nodularizer alloys. (a) RE-free, (b) 0.5%La, (c) 1.0%La, (d) 0.5%Ce, (e) 1.0%Ce, (f) 1.0%MM.

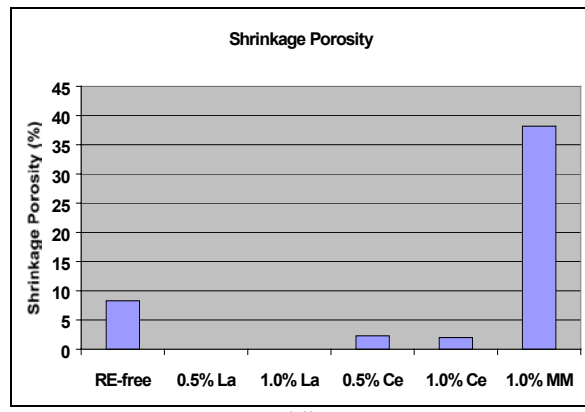
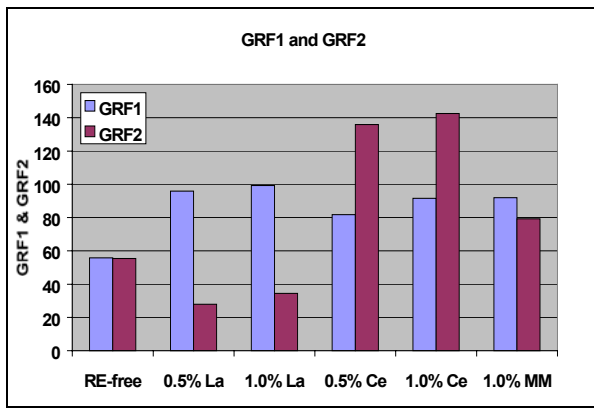
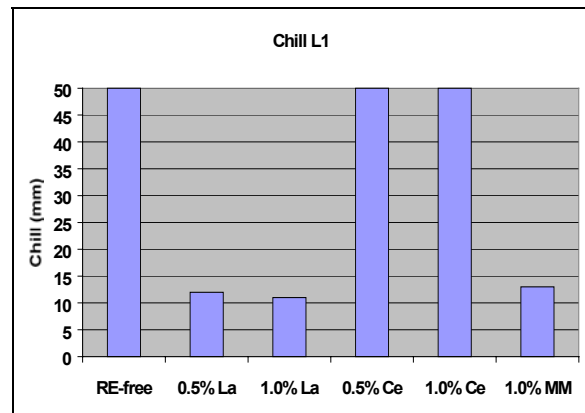
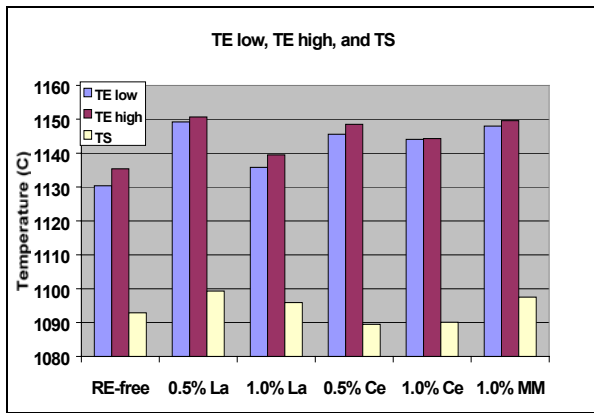


Figure 7: Characteristic ATAS thermal analysis data (TElow, TEhigh, TS, GRF1, GRF2), chill wedge carbides, and relative shrinkage porosity for the experimental castings.

SUMMARY

The following conclusions can be drawn from the present investigation:

- Nodule count is found to be 2 to 3 times higher for the pure lanthanum bearing MgFeSi alloy versus the pure cerium-bearing alloy in the ladle treatment process for ductile iron.
- Nodularity is increased by 10 to 20% with the lanthanum bearing MgFeSi alloy.
- The pearlite content is reduced up to 50% with the lanthanum containing alloy versus the pure cerium bearing alloy.
- Nodule size distribution is found to be more skewed to smaller sizes when using the pure lanthanum bearing nodularizer alloy.
- Chilling tendency is substantially lower when using pure lanthanum bearing MgFeSi, and for a 0.5% La-bearing alloy it is found that the 5 mm casting section is virtually carbide free in un-inoculated condition.
- Shrinkage porosity in a hot spot crossbar is found to be eliminated when using the pure lanthanum bearing MgFeSi alloy.
- Thermal analysis data support the metallographic findings of significantly reduced tendency for chill and shrinkage formation when using the pure lanthanum bearing MgFeSi nodularizer alloy in a ladle treatment process.

REFERENCES

1. Z. Bofan and E. W. Langer: Scand. J. of Metallurgy, 1984, 13, p15.
2. D. M. Stefanescu, S. K. Biswal, C. Kanetkar and H. H. Cornell: in Proc. Advanced Casting Technology, Kalamazoo MI, USA, Nov. 1986, p167.
3. U. H. Udomom and C. R. Loper, Jr.: AFS Transactions, 1985, 93, p519.
4. H. Itofuji and H. Uchikawa: AFS Transactions, 1990, 98, p429.
5. E. N. Pan, C. N. Lin and H. S. Chiou: Jpn Foundrymen's Soc. in Proc. 2 Asian Foundry Congress, 1994, p36.
6. P.C. Liu, T.X. Li, C.L. Li and C.R. Loper, Jr.: AFS Transactions, 1989, 97, p11.
7. M. J. Lalich: in Proc. 2nd int. symp. on the metallurgy of cast iron, Geneva, Switzerland, May 1974, p561.
8. C. S. Kanetkar, H. H. Cornell and D. M. Stefanescu: AFS Transactions, 1984, 92, p417.
9. M. I. Onsøien, Ø. Grong, T. Skaland and S.O. Olsen: AFS Transactions, 1997, 105, p147.
10. C.M. Dunks, "In-the-mould Worldwide – Today and tomorrow", AFS Transactions, 1982.